Planar optical array with a spatial-integration feature

Daniel Vázquez, Javier Alda, and Eusebio Bernabeu

A planar optical array is presented that provides a selective concentration of the light incident upon the system onto a given area. Several alternative designs are analyzed and explained geometrically. The photometric calculation is presented for three different levels of approximation. A prototype of the proposed system is tested, showing good accordance with the theoretical predictions. © 1999 Optical Society of America

OCIS codes: 040.1240, 080.2730, 080.2740, 100.2550, 230.0230.

1. Introduction

A spatial integrator can be defined as an optical system that collects light from any source located in front of it. A typical spatial integrator is formed when several individual optical units are placed side by side. Their cooperative parallel action produces the desired spatial-integration behavior. Theoretically, an integrator produces a uniform and well-defined light spot on a given plane. Within the formalism of optical arrays, this spot is called the synthetic image.[1] In these systems the light enters the individual units through their apertures. These apertures are imaged by the optical system behind them onto the synthetic image. The relative misalignment of each individual unit is calculated to make individual images of the apertures coincide and produce the synthetic image. Therefore any light entering the aperture of the individual unit and reaching the output plane of the unit will be forwarded to the synthetic image and will produce the integration feature. This property can be used in several applications. The architectural design of natural lighting systems is maybe one of the most obvious fields for application of these devices. Optical sensors, able to detect a given signal without regarding the spatial location of the source, could be improved by use of an appropriate spatial integrator such as one of those described in this paper. In contrast, the planar geometry presented here makes the fabrication and setup of the system simpler.

The framework of the theory of optical arrays was developed by Wang and Ronchi several years ago.[1] They proposed a simple and clear treatment based on matrix optics. The units of the array are described by their *abcd* matrix, and some transformation rules are applied to obtain the *abcd* matrix of the array. The elements of the *abcd* matrix that characterized an optical array having a spatial-integration feature comply with the following relation,

$$R = l - b/d, \tag{1}$$

where R is the distance between the input plane of the array and the synthetic image plane, l is the length of the individual optical unit, and b and d are the elements of the matrix of each unit of the optical array. This condition implies that the optical axis of each individual unit intersects at the center of the synthetic image. A typical configuration already proposed by Wang and Ronchi[1] locates the vertex of the input optical element on a spheric surface with radius R, whose center is also the center of the synthetic image. This arrangement produces a spherical dome configuration. In some previous research[2–4] we proved the feasibility of this system to produce a uniform shadowless illumination on a given area whose size, shape, and position can be easily calculated. In that case we followed a typical procedure, using a sphere to locate and align the axis of the individual units of the array. For practical reasons the spheric dome solution is not easily integrated into architectural design and into other areas of optical design, where these optical integrators

When this research was performed D. Vázquez and J. Alda were with the Department of Optics, University Complutense of Madrid, Escuela Universitaria de Óptica, Avda, Arcos de Jalón, s/n. 28037 Madrid, Spain. E. Bernabeu was with the Facultad de Físicas, Ciudad Universitaria, s/n. 28040 Madrid, Spain. J. Alda is currently with the Center for Research and Education in Optics and Lasers, University of Central Florida, P. O. Box 162700, Orlando, Florida 32816-2700 (e-mail for J. Alda, j.alda@fis.ucm.es).

Received 28 July 1998; revised manuscript received 30 October 1998.

0003-6935/99/071133-06$15.00/0

could prove their advantages. Therefore we propose a planar arrangement in which the individual optical units are located on a plane and designed specifically to meet the requirements of the spatial integrators.

In Section 2 the basic ideas of the design of the planar array are described and justified. In Section 3 a practical example is analyzed by numerical evaluation of the photometric behavior of the system. The experimental setup of a planar array is described in Section 4, where the characteristic parameters of the array are tested.

2. Design of a Planar Spatial Integrator

The basic theory of optical arrays is made within the paraxial approach. Wang and Ronchi[1] used matrix optics to develop a solid framework where the optical arrays can be included. In this treatment the individual units of the array are described by a 2×2 *abcd* matrix, which is extended to a 4×4 matrix when the misalignment and decentration of the units are taken into account. This misalignment and decentration are represented by the height and slope of the optical axis of the individual unit at the input plane of the array. Therefore the location and orientation of the optical axis become crucial parameters of the design. Actually, one of the key factors in the manufacture of spatial integrators is to align the optical axis of the individual units to make them coincide at the center of the synthetic image. In contrast, the optical axis of the spatial integrator can be obtained when a perpendicular line is traced from the center of the synthetic image.

An interesting property that follows from Eq. (1) is that spatial integration does not depend on the a and c elements of the matrix characterizing the individual optical units of the array. When the system is made of actual elements, such as thick lenses or a pair of lenses, this means that the characteristics of the first element do not affect the integration feature.

The paraxial approach neglects the axial displacement of the input plane of the misaligned elements. All of them will coincide with the input plane of the whole array (see Fig. 1). By using this fact, we can design an optical array having the vertex of the individual elements on a planar surface. Every optical element is aligned in such a way that the optical axis of each of them coincides at the center of the synthetic image. So we would have an actual planar array with spatial-integration behavior.

It is interesting now to recall some concepts related to the use and definition of the optical axis of an optical system. The optical axis of a system composed of spherical surfaces is defined by a line joining the centers of curvature of the surfaces. In addition, a light ray that follows the optical axis remains undeviated as it passes through the system. The optical center is also defined as having the property that every light ray that passes through it comes out parallel to the input ray. Within the paraxial approach, a thin lens is a useful simplification of a thick lens. Every thin lens has its own optical axis and optical center. The optical axis is located in the same position as the optical axis of the corresponding thick lens. The optical center defines the position of the lens along the axis. The input plane of the system is perpendicular to the optical axis. An aligned optical system has a common optical axis for every individual optical element. A misaligned optical system can be seen as a composition of individual elements whose axes do not coincide. For a misaligned composition of thin lenses, we define the optical axis as the line that joins the optical centers of the individual lenses. Our planar array is constructed by use of this concept.

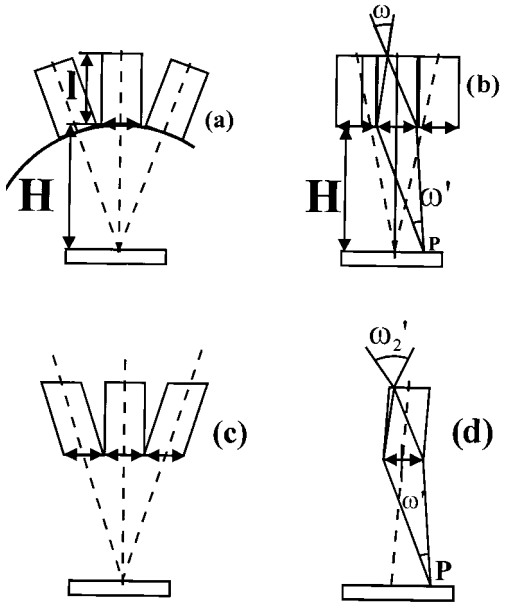

Fig. 1. Paraxial arrangement of the input planes for optical arrays, showing the equivalence of the systems: (a) Spheric dome solution; (b) lateral displacement of the second element (prismatic effect array); (c) lateral displacement of the aperture position (inclined array); (d) effect of a negative lens at the input plane.

The individual units of the planar array are made of a couple of simple elements. Each one has its own optical axis. For every unit, these two axes do not coincide (except for the central element of the array whose axis is the optical axis of the array) and are displaced laterally by a given amount, $\varepsilon_{\text{local}}$, remaining parallel to each other and, therefore, allowing a planar arrangement. If we define the optical axis of the individual unit of the array by joining the optical centers of these two optical elements, this misaligned optical axis has a slope given by

$$\varepsilon_{\text{local}}{}' = \frac{\varepsilon_{\text{local}}}{l}, \tag{2}$$

where l is the length of the individual element.

The spatial-integration feature is obtained when the optical axes of every unit coincide at the center of the synthetic image. This condition is fulfilled by a progressive decentration of the components of the individual element of the array as we move farther

from the optical axis of the whole array. The decentration is described by the following relation:

$$\varepsilon' = \varepsilon/R, \tag{3}$$

where ε represents the position of the center of the first optical element of the individual unit of the array with respect to the optical axis of the array and R is the distance between the input plane of the array and the synthetic image plane. Because the optical axis of the array is parallel to the optical axis of the components of the individual elements of the array, we find that $\varepsilon' = \varepsilon_{\text{local}}'$. Let us assume that the optical array is made of individual units composed of two elements, for example, two lenses. The input and the output elements of each unit are regularly spaced by two periods, p_1 and p_2, respectively. The lateral displacements with respect to the optical axis of the array can be given as a function of the order, $j = 0, \pm 1, \pm 2, \ldots$, with respect to the central element as

$$\varepsilon_1(j) = jp_1, \qquad \varepsilon_2(j) = jp_2, \tag{4}$$

and the slope becomes

$$\varepsilon'(j) = j\frac{p_1 - p_2}{l}, \tag{5}$$

which must obey Eq. (3).

This decentration can be obtained by several equivalent procedures. One of them uses the prismatic effect produced by a lens whose optical axis is moved laterally. Furthermore, the array is constructed by an actual decentration of the components [see Fig. 1(b)]. This arrangement allows the units to be stacked side by side with parallel walls fitting the optical element and with its axis properly displaced into its frame. This local decentration can be expressed for the second element of the two-element arrays as

$$\varepsilon_{2_{\text{local}}}(j) = -j(p_1 l/R), \tag{6}$$

where the minus sign indicates that the displacement is toward the center of the optical array. The characteristics of the first element of the array are left free for other design conditions. For example, the field of view of the individual elements can be increased by use of an appropriate negative value of the focal length of the first element. This negative lens would also help to homogenize the illuminance on the synthetic image [see Fig. 1(d)]. It would be possible to align the optical axis of the individual elements to intersect at the synthetic image plane by decentering the first element. However, this option would not work, because the imaging properties of the second lens that produce the synthetic image would not be fulfilled.

Another option is to displace the position of the center of the elements of the individual unit by keeping them centered within their frames [see Fig. 1(c)]. The prototype constructed by us is based on this configuration. The relative displacement between elements is also given by Eq. (4). The condition to comply with the spatial-integration feature is given by the following equivalent relations:

$$\varepsilon'(j) = j\frac{p_1 - p_2}{l} = j\frac{p_1}{R} = j\frac{p_2}{R - l}. \tag{7}$$

In our case the first element is a simple aperture. For this element the significance of the optical center could be lost. We have chosen the geometrical center of the aperture as this optical center. The integrator is made with individual elements whose axis are equispaced by an angle,

$$\alpha = \frac{p_1 - p_2}{l} = \frac{p_1}{R} = \frac{p_2}{R - l}. \tag{8}$$

3. Photometric and Radiometric Efficiency

Here we simulate numerically the proposed system to study some photometric and radiometric parameters that should inform us about the quality of the illumination on the synthetic image.

First we need to characterize and locate the position and size of the diaphragms of the system. From the synthetic image plane, the aperture diaphragm is the frame of the lens located at the exit plane of the individual element. The field diaphragm is the input aperture of the individual element. This input aperture is also the entrance window, and the synthetic image is the exit window itself. Then the spatial integration can be seen as a superposition of the exit windows on a given position where the synthetic image is located. If we move to the center of the aperture diaphragm, we can see the field of view of each individual element. This field of view is determined by the rim of the aperture of the first element. We can increase the field of view by introducing a negative lens into the first surface, as we proposed in Section 2. The effect of this lens can be known when the center of the aperture diaphragm is imaged with the negative lens [see Fig. 1(d)].

In order to get more insight into the radiometric efficiency of the system, we propose three methods of calculation to get the desired information. For all of them the geometric, radiometric, and photometric parameters are calculated for circular pupils and diaphragms.

The first one uses an average method. The wide tolerance, which can be taken in most of the architectural applications and in the data of natural lighting, allows us to apply this method. In this model the illuminance on the exit pupil is assumed to be uniform. We have assumed a uniform source with a luminance L that accurately models the cloudy sky in daytime. Other calculations have been made for clear sky. This average method is applied in two particular cases: when the optical element can be considered a thin optical element (thin with respect to the distance between the element and the synthetic image plane), and when the luminance of the sources inside the field of view of the element varies smoothly, for example, for daylight from covered sky.

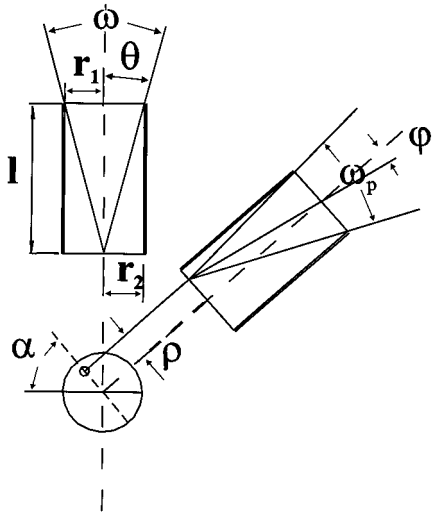

Fig. 2. Geometry for the calculation of the solid angle subtended by each element of the array.

Within these assumptions the illuminance on the exit pupil, E_m, is given by

$$E_m = \omega_m L, \tag{9}$$

where ω_m is the average solid angle and L is the source luminance. The luminous flux given by each element is

$$\Phi_u = \omega_m L \pi {r_1}^2, \tag{10}$$

where r_1 is the radius of the circular input aperture of the element. The illuminance at a given point of the synthetic image plane is

$$E = \frac{\Phi_T}{A} = \frac{N\Phi_u}{A} = \frac{N\omega_m L \pi {r_1}^2}{A}, \tag{11}$$

where N is the number of elements of the array and A is the area of the synthetic image. Therefore the illuminance on the synthetic image is

$$E_i = \frac{4NL\omega_m r^2}{d^2}, \tag{12}$$

where d is the synthetic image diameter. (If the input aperture has a circular shape, then the synthetic image will be a magnified image of it.)

A second method estimates the luminous flux through the exit pupil. This estimation must be done when the previous assumptions about the uniform luminance are not fulfilled or when elements are close to the synthetic image and the solid angle varies significantly for different positions along the synthetic image. In Fig. 2 we show the geometry of the situation. Let $\omega = 2\pi(1 - \cos\theta)$ be the solid angle seen from the center of the last diopter of an individual element. Then the solid angle seen from any other point of this last diopter could be written as

$$\omega_p = \omega \cos\phi = \omega \frac{l}{(l^2 + \rho^2)^{1/2}}.$$

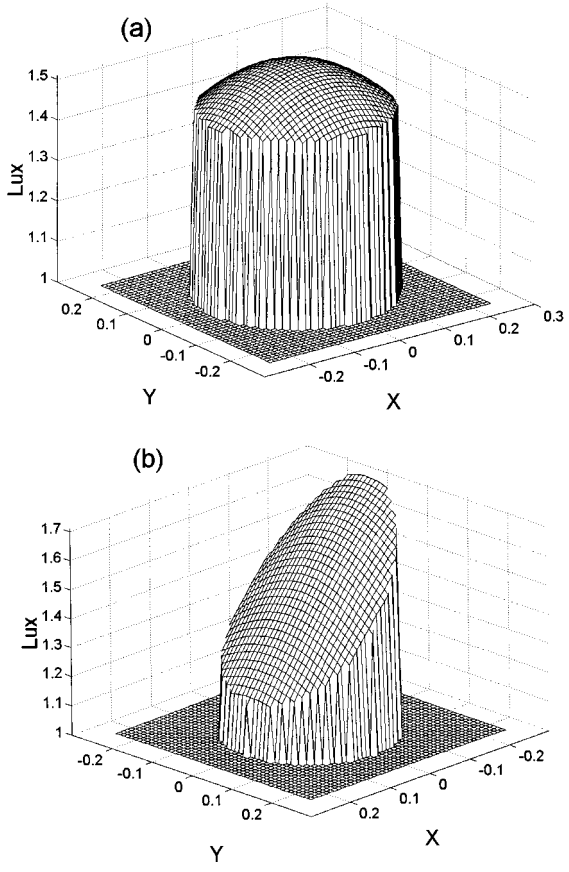

Fig. 3. Simulated illuminance distribution on the synthetic image plane for a 4×4 spatial integrator (X and Y axes are in meters). The parameters of the array are $r_1 = 0.029$ m, $1/f' = 7.25$ m^{-1}, and $R - l = 1$ m. (a) Constant luminance conditions; (b) clear sky conditions with the Sun located at 45° of elevation.

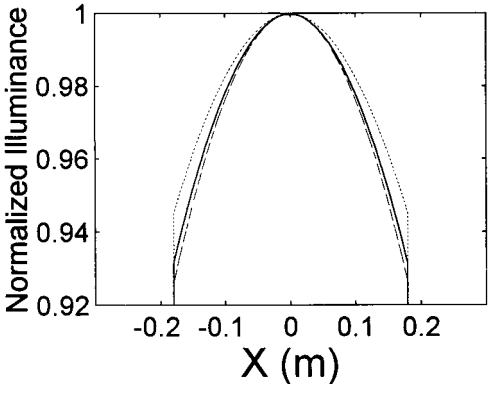

Fig. 4. Dependence of the illuminance distribution with respect to the number of elements in the array. The dashed curve corresponds to an individual unit, the solid curve is for a 5×5 arrangement, and the dotted curve is for 10×10 array. Note that the illuminance range is normalized to the maximum of the distribution for each case. Therefore this graph shows how the homogeneity of the illuminance distribution increases with the number of elements.

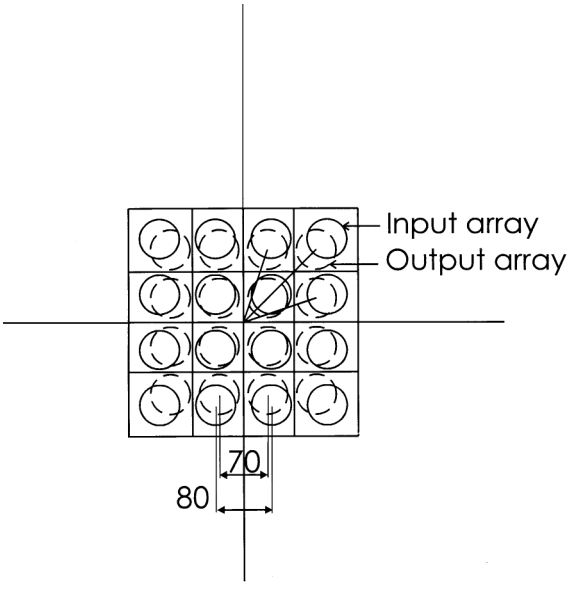

(a)

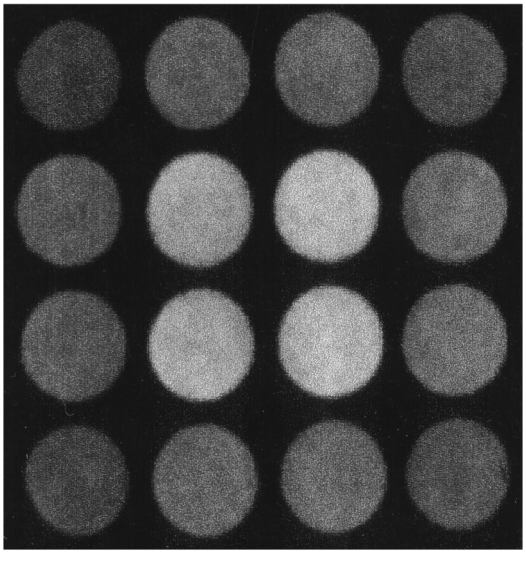

(b)

Fig. 5. Prototype configuration of a planar spatial-integrator array: (a) frontal view of the system, showing the input and output planes and apertures for every unit (numbers in millimeters); (b) photograph of the back side of the prototype, showing the circular apertures that contain the lenses.

The luminous flux is $\Phi_u = \int_{A_2} \int_\Omega L \mathrm{d}A_2 \mathrm{d}\omega$, which for a constant exterior luminance provides that

$$\Phi_u = \int_0^{r_2} \int_0^{2\pi} L\omega \frac{l}{\sqrt{l^2 + \rho^2}} \rho \mathrm{d}\rho \mathrm{d}\alpha = 2\pi L\omega l[(l^2 + r_2^{\,2})^{1/2} - l]. \quad (13)$$

The third approach is a more exact calculation that can be done with a point-to-point calculation. In this case the illuminance on the synthetic image is $E_p(j) = L_o \omega_p \cos(j\alpha)$, where ω_p is the solid angle seen from the point P on the synthetic image plane (this angle can be deduced within the paraxial approach), and α is the angle between the axis of adjacent units. If the outside luminance is constant, the calculation becomes simpler. The solid angle ω_p can be deduced within the paraxial approach. The total illuminance will be obtained at every point P, adding the contribution of every array unit and changing j.

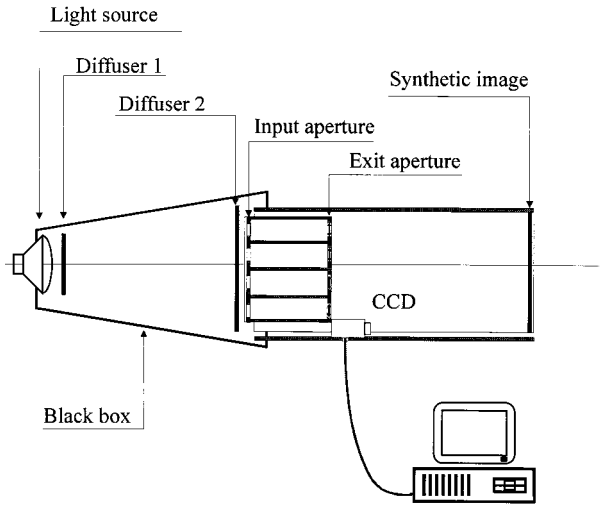

Fig. 6. Scheme of the experimental setup used to measure the synthetic image.

Figure 3(a) shows the simulated illuminance distribution on the synthetic image plane when the source luminance is constant, $L = 1$ cd/m^2, obtained for an array of 4×4 elements whose parameters are those of the prototype constructed by us and described in Section 4. In Fig. 3(b), we have plotted the simulated illuminance for the same array with its optical axis vertical, clear sky conditions, and the Sun located at 45° of elevation. A larger number of units in the array improves the uniformity of the illuminance distribution at the same time that increases its absolute value. In Fig. 4 we have plotted these changes for several configurations with an increasing number of elements.

4. Experimental Results

To test the behavior of the planar solution proposed in this paper, we have constructed a spatial-integrator array (see Fig. 5). Each individual element is composed of a circular aperture, a tube, and a lens. The arrangement of the elements corresponds to the case shown in Fig. 1(b). The optical parameters of the array are $1/f' = 7.25$ m^{-1}, $R - l = 1$ m, and $l = 0.16$ m. The transverse dimensions are $r_1 = r_2 = 0.029$ m. The individual elements are located in a rectangular arrangement of 4×4. The lenses are mounted on a flat surface whose circular openings are on a rectangular grid of period $p_2 = 0.070$ m. The input apertures are also on a planar rectangular grid with period $p_1 = 0.080$ m. The difference between both spatial periods, along with the length of the optical elements, produces an equiva-

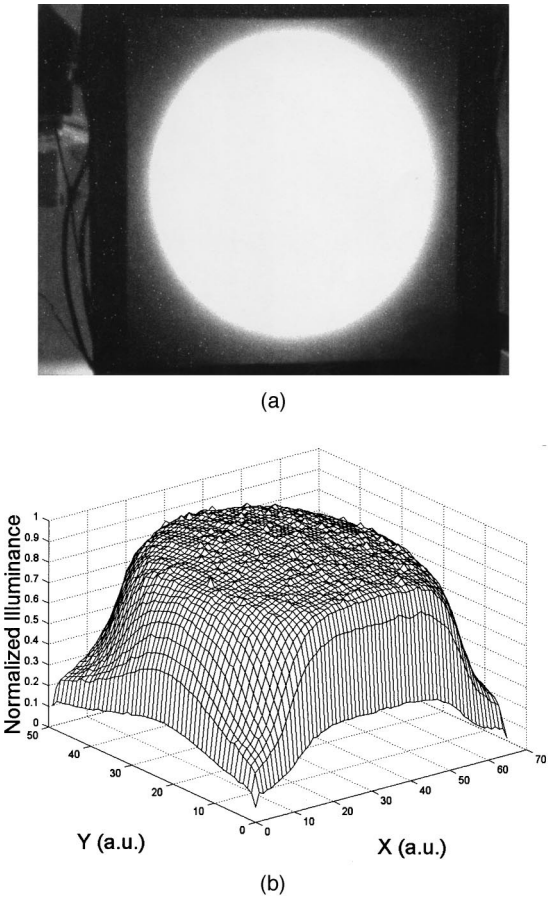

Fig. 7. Synthetic image distribution: (a) photograph of the synthetic image seen from the outside of the experimental setup; (b) three-dimensional illuminance distribution seen by the CCD from the position indicated in Fig. 6.

lent spherical array whose radius is $R = 1.16$ m, which coincides with the distance between the input plane and the synthetic image plane.

We have performed several measurements of the local illuminance obtained at the synthetic image plane for uniform outside luminance by using the arrangement of Fig. 6. In the experimental setup the array is placed in front of a white-light source that illuminates a diffusing screen located on the input plane of the array. The light distribution on the synthetic image plane is obtained with a CCD camera and a framegrabber whose linearity is ensured.[5] Figure 7 shows one of the synthetic images obtained and its three-dimensional plot of the illuminance distribution. In Fig. 8 we present the measured illuminance distribution (in arbitrary units) obtained along a diameter of the synthetic image, which shows good agreement with the simulated values obtained in Section 3.

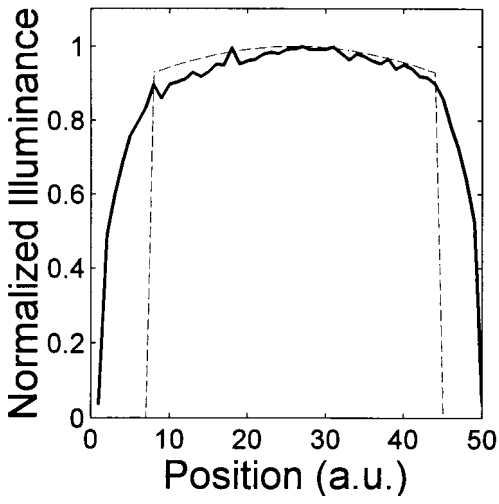

Fig. 8. Plot of the experimental illuminance distribution (solid curve) on the synthetic image plane along one of the diameters of the image, compared with the simulated results (dashed curve).

5. Conclusion

We have shown several solutions for the construction of planar spatial integrators. These solutions have been analyzed by use of simple geometrical optics tools. A prototype of the system has been constructed and tested. The experimental data coincide well with the theoretical and numerical predictions presented in this paper.

We are very grateful to Felix González and Diego Castillo for their help in building the prototype. We also thank Antonio Quiroga and Héctor Canabal for his assistance in the image acquisition of the synthetic image. This research was partially supported by project MAT-95-0767 of the Comisión Interministerial de Ciencia y Tecnología of Spain. This research was finished during a stay by one of the authors (J. Alda) at the Center for Research and Education in Optics and Lasers (CREOL, University of Central Florida, Orlando, Florida). This stay was supported by the Ministerio de Educacion y Cultura of Spain and by a grant from CREOL.

References

1. S. Wang and L. Ronchi, "Principles and design of optical arrays," *Prog. Opt. XXV*, 279–348 (1988).
2. J. Alda, H. Kamal, and E. Bernabeu, "Optimum design of optical arrays with spatial integration feature," Opt. Eng. **36,** 2872–2877 (1997).
3. H. Kamal, "Design and properties of optical arrays," PhD. dissertation (Universidad Complutense de Madrid, Spain, 1998).
4. D. Vázquez and E. Bernabeu, "Array optical device for natural lighting," *Light. Res. Technol.* **29,** 33–39 (1997).
5. J. A. Quiroga, A. González, and E. Bernabeu, "Fast method to measure the irradiance response of an image processing system," Meas. Sci. Technol. **6,** 181–187 (1995).